Fabrication of Near-Infrared Photonic Crystals Using Highly-Monodispersed Submicrometer SiO_2 Spheres

Wei Wang,*,† Baohua Gu,† Liyuan Liang,†,§ and William A. Hamilton‡

Environmental Sciences and Condensed Matter Sciences Divisions, Oak Ridge National Laboratory, P.O. Box 2008, Oak Ridge, Tennessee 37831, and School of Engineering, Cardiff University, P.O. Box 925, Cardiff CF24 0YF, U.K.

Received: January 21, 2003; In Final Form: June 25, 2003

Silica (SiO_2) spheres with diameters of 400−850 nm were prepared by hydrolysis of tetraethyl orthosilicate (TEOS) in the presence of water and ammonia in an alcoholic medium. By grafting $-SO_3^-$ groups on silica surfaces using the silane coupling agent, 2-(4-chlorosulfonylphenyl) ethyltrimethoxysilane, surface charges of the SiO_2 spheres were greatly enhanced. These highly charged, monodisperse SiO_2 particles readily self-assemble into robust, three-dimensionally ordered crystalline colloidal array (CCA) photonic crystals in water suspension. By evaporating water in the CCA, high quality films of close-packed SiO_2 particle−air arrays form with thickness of 25−125 μm. These SiO_2 CCAs and close-packed SiO_2 particle−air arrays diffract light in the near-infrared (NIR) spectral region according to Bragg's law. By altering the particle number density in the CCA dispersions, the diffraction wavelength can be continuously tuned from ∼800 to ∼1800 nm. Additionally, the diffraction prevented light from transmitting through the CCA and the close-packed SiO_2 particle−air array below ∼550 nm spectral region. The CCA photonic crystal materials could be potentially used as tunable NIR optical filters and/or as photonic band gap materials in the UV−visible spectral region.

I. Introduction

Materials with spatially ordered features on the mesoscale of 50−500 nm have important applications in optical information processing and storage, advanced coatings, catalysis, spectroscopic instrumentation, and other emerging nanotechnologies.[1−5] Colloidal photonic crystals, which diffract light according to Bragg's law, are a promising class of such materials. In particular, soft colloidal photonic crystals, known as crystalline colloidal arrays (CCAs), are formed by non close-packed, three-dimensional arrays of colloidal spheres in suspensions, where the lattice spacing is much greater than the particle diameter itself. The CCAs form via self-assembly of particles into crystalline arrays in a size range from nanometers to micrometers, and they exhibit unusual optical[2,6−8] and thermodynamic properties.[9−11] These unique properties give the CCAs applications in optics and spectroscopic instrumentation;[12] furthermore, functionalized and immobilized CCAs are used to create chemical sensing materials.[2]

While the colloidal crystals, mostly composed of polymer colloids such as polystyrene, with diffraction properties in the UV and visible regions have been extensively studied, it is a great challenge to obtain colloidal crystals that operate in the near-infrared (NIR) wavelength range. Recently, Asher et al.[13] has developed a NIR photonic crystal using highly charged polystyrene latex colloids. However, there is no report for SiO_2 photonic crystals with diffraction wavelength above 1500 nm.[14−17] To Bragg-diffract light in the NIR region, the array spacings in the CCA have to be large enough. For example, by diluting particle concentration, the CCA diffraction peak may extensively shift from the UV−visible to the NIR region. However, a great challenge here is that the volume fraction of particles in the diluted CCA becomes so low that CCA diffracts light inefficiently and is susceptible to disorder because of a weak electrostatic repulsive force between the colloidal spheres. It is therefore necessary to produce large colloidal spheres and to enhance their surface charge density in order to successfully prepare a CCA that diffracts light in the NIR region. In this report, we present a procedure to prepare large SiO_2 spheres (400−850 nm) with a high monodispersity and surface functionalized with silane coupling agent to maximize its surface charge density. For the first time, we successfully fabricated SiO_2 CCAs, which diffract light at wavelength >1500 nm in the NIR region.

II. Experimental Section

Materials. Tetraethyl orthosilicate (TEOS, ≥99%) and $NH_3 \cdot H_2O$ (29.4%) were obtained from Fluka and J. T. Baker, respectively. The 2-(4-chlorosulfonylphenyl) ethyltrimethoxysilane (CSPETMOS) was from United Chemical Technologies. Absolute ethanol, chloroform, 2-propanol (99.5%), and NaOH solution (1 N) came from EM Science. All chemicals were used as received. SnakeSkin pleated dialysis tubing with a molecular weight cutoff at 10 000 was purchased from Pierce Chemical Company. The AG 11 A8 ion-exchange resin (mixed bed) was a Bio-Rad product. Deionized water with a resistivity of >18.0 MΩ cm was obtained from a Millipore-Q Plus water purifier and used throughout the experiment.

Synthesis. Monodisperse SiO_2 spheres were prepared by hydrolyzing TEOS in an alcoholic medium in the presence of water and ammonia using a modified procedure originally described by Stöber et al.[18] Typical preparation is to rapidly mix two equal-volume parts with a total volume of ∼250 mL—one includes alcohol and TEOS, while another one includes alcohol, water, and ammonia. Fixed concentrations of 17.0 M H_2O and 1.63 M NH_3 were used for the synthesis of SiO_2

* Corresponding author. E-mail: wangw@ornl.gov.
† Environmental Sciences Division, Oak Ridge National Laboratory.
‡ Condensed Matter Sciences Division, Oak Ridge National Laboratory.
§ Cardiff University.

10.1021/jp034161b CCC: $25.00
Published on Web 10/11/2003

TABLE 1: Size, Surface Charge Density, and ζ Potential of SiO_2 Spheres Prepared at $[NH_3] = 1.63$ M, $[H_2O] = 17.0$ M

property	sample ID			
	S-1	S-2	S-3	S-4
D (nm) ± polydispersity				
TEM	403 ± 3.7%		620 ± 3.4%	
DLS	429 ± 8.1%	545 ± 7.7%	648 ± 4.3%	841 ± 6.0%
[TEOS] (M)	0.2	0.2	0.3 + 0.3[a]	0.3 + 0.3[a]
solvent	2-propanol	ethanol	2-propanol	ethanol
titrated charge density ($\mu C/cm^2$)[b]				
before surface modification		0.24		0.16
after surface modification		0.94		0.88
ζ potential (mV) ± half width (mV)				
before surface modification	−50.0 ± 4.1	−52.5 ± 7.6	−55.7 ± 8.6	−50.6 ± 5.1
after surface modification	−68.9 ± 6.0	−67.4 ± 5.3	−65.4 ± 4.5	−62.6 ± 6.4

[a] Two-step TEOS addition, as described in the text. [b] Surface charge and ζ potential were measured using purified colloidal suspensions in deionized water; silane coupling agent, CSPETMOS, was used for the surface modification.

particles, and the resulting particle sizes were controlled by varying TEOS concentration and solvent (ethanol or 2-propanol). Depending on the solvent type and the TEOS concentration, the reaction mixture appeared to be turbid white in 2−15 min, as SiO_2 particles were formed. The reaction was allowed to continue for 6 h with moderate stirring at room temperature for full completion.

After the hydrolysis and condensation of TEOS were complete, about 1−2 mL of 50% CSPETMOS (CH_2Cl_2 solution) was added dropwise into the colloidal suspension to react with SiO_2 surfaces and therefore to modify the surface properties of SiO_2 spheres. After addition of CSPETMOS, the reaction was allowed to continue for an additional 12 h with vigorous stirring. When the functionalization reaction was completed, the SiO_2 particles were separated by centrifugation, washed with ethanol, and then washed with deionized water. In these cleaning cycles, a vertex mixer and an ultrasonication bath were used to redisperse the particles in the desired solvents, and centrifugation was used in every step of the solid−liquid separation.

Measurements. Transmission electron microscopy (TEM) images were taken with a Hitachi HF-2000 electron microscope operated at 200 kV. Sample particles were placed on carbon/formvar film supported by a copper grid (Ted Pella, Inc.). The average particle size, D, and the standard deviation, σ, were determined by digitizing the printed micrographs and analyzing 300 particles using the public domain NIH Image 1.60 software (http://rsb.info.nih.gov/nih-image/). The polydispersity from the TEM image is defined as σ/D.

The particle size and polydispersity of colloidal nanoparticles were also examined by dynamic light-scattering (DLS) measurement using a Brookhaven Zeta PALS analyzer. Purified colloidal particles were dispersed in deionized water for the measurement.

Optical transmission spectra were obtained using a Perkin-Elmer Lambda 9 UV/VIS/NIR or a Hewlett-Packard 8453 spectrophotometer. Quartz cells with 25−125 μm spacer were used for all the measurements.

Surface charge densities on the hydrophilic SiO_2 colloidal particles were measured by titrating the colloidal dispersion with standardized NaOH solutions, and the endpoint was determined by conductivity measurements using a conductivity meter. In principle, the total amount of the titratable charge groups ($\equiv SiO^-$ and $\equiv SO_3^-$) is equivalent to the amount of NaOH added when minimum conductivity is reached.[19]

III. Results and Discussion

Colloid Synthesis. A key element to successfully produce CCAs is the preparation of highly monodispersed colloids, which generally relies on the manipulation of the solution chemistry during colloid synthesis. It is well-known that the particle size and the polydispersity of synthesized SiO_2 particles strongly depend on reaction conditions, including the relative concentrations of TEOS, water, and ammonia,[8] the solvent type,[20] and the temperature.[21] The fabrication of monodisperse SiO_2 spheres (<400 nm) have been studied extensively,[22−24] but most of the published recipes give relatively high polydispersity for the SiO_2 spheres with diameters > 400 nm, which is not good enough for the CCA fabrication. We systematically varied the reaction parameters in order to generate large SiO_2 spheres rapidly with minimal polydispersity. As shown in Table 1, colloidal SiO_2 particles in the size range from 400 to 850 nm have been obtained by varying the TEOS concentration or the type of solvents at fixed ammonia and water concentrations.

Results indicate that the use of different types of organic solvents remarkably affect the size of synthesized SiO_2 spheres. Larger particles were synthesized in ethanol than in 2-propanol as a solvent. The volume of the growing particles increased in proportion to the number of moles of TEOS added to the solution; however, when the TEOS concentration is >0.3 M, the resulting particles exhibit a high polydispersity because of inhomogeneous nucleation or particle agglomeration in the one-step growth process. To obtain SiO_2 spheres with both large particle size and high monodispersity, we used a two-step growth technique as follows. First, an aliquot of the TEOS was added to the solution to form a seed suspension at a concentration of 0.3 M TEOS. After 20 min, the remaining TEOS was added a drop at a time at a rate of ∼1 mL/min. The slow addition of the second part of TEOS does not cause formation of new nuclei of colloidal particles. This implies that during the ensuing hydrolysis and condensation with the addition of remaining TEOS, the number of colloidal particles remains constant but their size increases. This two-step synthesis process is therefore successful in producing large SiO_2 spheres with a high monodispersity. Figure 1 shows typical TEM images of the SiO_2 colloids synthesized by the one- and two-step procedures. Both TEM and DLS measurements indicate that SiO_2 colloids are highly monodispersed (Table 1). Note that the particle sizes measured by DLS are generally larger than those obtained from TEM. This is because the highly purified SiO_2 colloids have a thick electric double layer in deionized water, while the DLS measurement reflects the hydrodynamic size of the colloids. These particles carry a net negative surface charge ranging from −50 to −56 mV as determined by the ζ potential measurement, or from 0.16 to 0.24 $\mu C/cm^2$ as determined by the surface charge titration (Table 1).

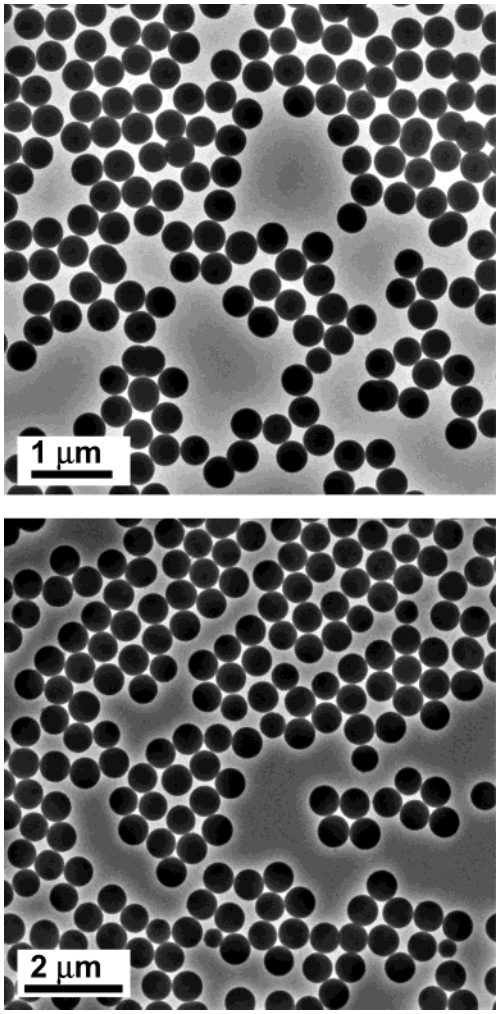

Figure 1. TEM images of SiO_2 spheres prepared by (a) one-step process ($D = 403$ nm, $\sigma = 15.1$ nm, polydispersity = 3.7%), and (b) two-step process ($D = 620$ nm, $\sigma = 21.3$ nm, polydispersity = 3.4%).

Surface Modification for Charge Enhancement. As stated earlier, the ionization of the SiO_2 surface hydroxyl groups gives negatively charged particles. Because the silanol groups are weakly acidic, they only partially dissociate in pure water.[25] The ζ potentials of these colloids are about -53 mV on average, and the surface charge densities are ~ 0.2 $\mu C/cm^2$ (Table 1). Under these conditions, the surface charges of the SiO_2 spheres are usually not sufficient for particles to self-assemble and to form robust colloidal crystal arrays in suspension. To maximize electrostatic interactions between the SiO_2 spheres to form robust colloidal crystalline phases, maximizing SiO_2 surface charge density is necessary and done by surface modification using the silane coupling agent CSPETMOS. The silane coupling agent was grafted onto the SiO_2 surface via hydrolysis of its methoxy groups, while $-SO_2Cl$ groups are hydrolyzed to give negatively charged $-SO_3^-$ groups. The attachment of the silane coupling agent on SiO_2 surfaces was evidenced by comparing UV spectra taken before and after the surface modification for purified colloids (Figure 2). The UV absorption peak at 225 nm is indicative of the presence of aromatic ring groups of CSPETMOS bonded on silica surfaces. As shown in Table 1, the ζ potential and surface charge density increased to about -65 mV and 0.9 $\mu C/cm^2$ after the surface modification. The charge densities on SiO_2 sphere surfaces are therefore enhanced by nearly 5 times through the surface modification process.

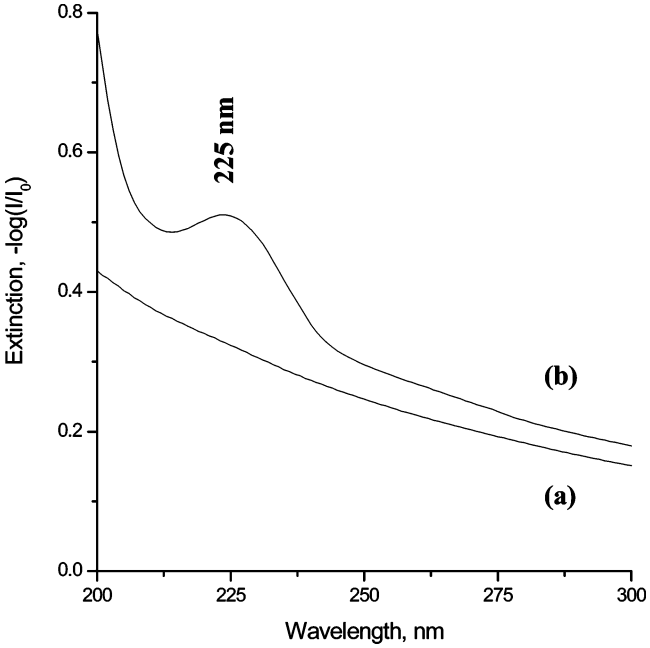

Figure 2. Extinction spectra of SiO_2 colloids (a) before and (b) after surface modification using a silane coupling agent, 2-(4-chlorosulfonylphenyl) ethyltrimethoxysilane (CSPETMOS).

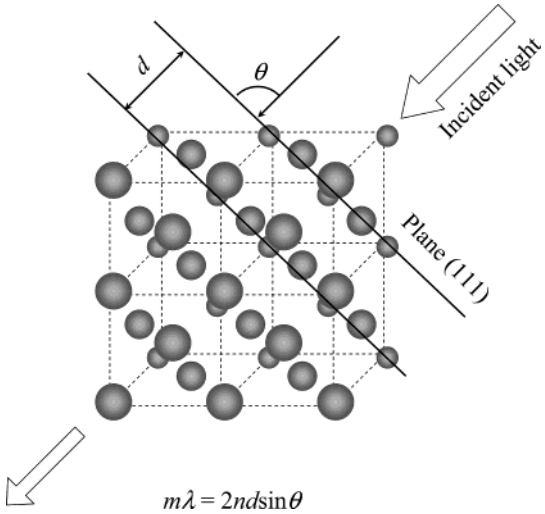

Figure 3. Schematic drawing of Bragg diffraction of CCA with face-centered cubic structure.

NIR Photonic Crystals. Highly charged, monodispersed colloidal spheres self-assemble in solution into CCAs, where the lattice spacings are much larger than the sphere diameters. These charged particles electrostatically repel each other, and the system minimizes its free energy by self-assembling into either a body-centered cubic (BCC) or a face-centered cubic (FCC) lattice.[26−34] Theoretical calculations indicate that the FCC structure is slightly more stable than the BCC structure.[34] Figure 3 is an illustration of the diffraction phenomenon from the (111) planes of CCA with FCC arrangement. However, it must be pointed out that small amounts of ionic impurity may screen repulsive interactions between the colloidal particles and thus "melt" the CCAs. To maximize the electrostatic repulsive force, these charged and functionalized colloidal particles were further purified by dialysis against deionized water to exchange remaining nonaqueous solvent molecules and remove any solvated impurities. During the dialysis, water was changed daily until its conductivity showed no further changes. Additionally, the resulting colloidal suspension was added with a mix-bed

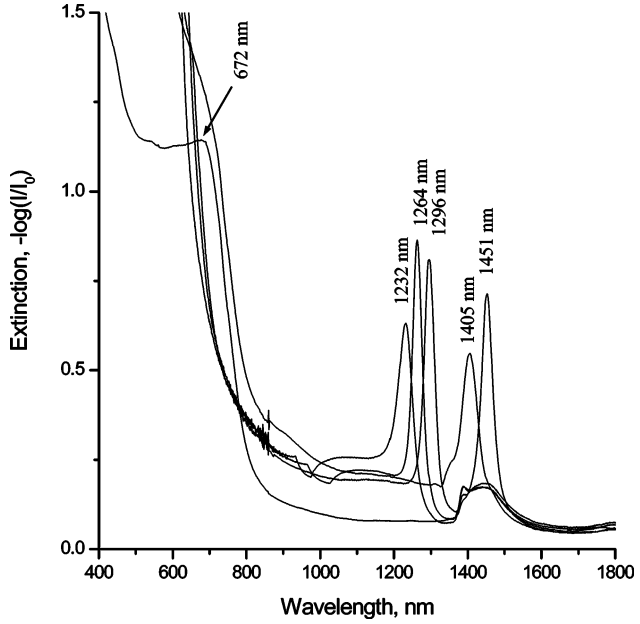

Figure 4. Normal incident extinction spectra of a 125-μm-thick CCA at different particle concentrations. The SiO_2 colloidal spheres are about 403 nm in diameter.

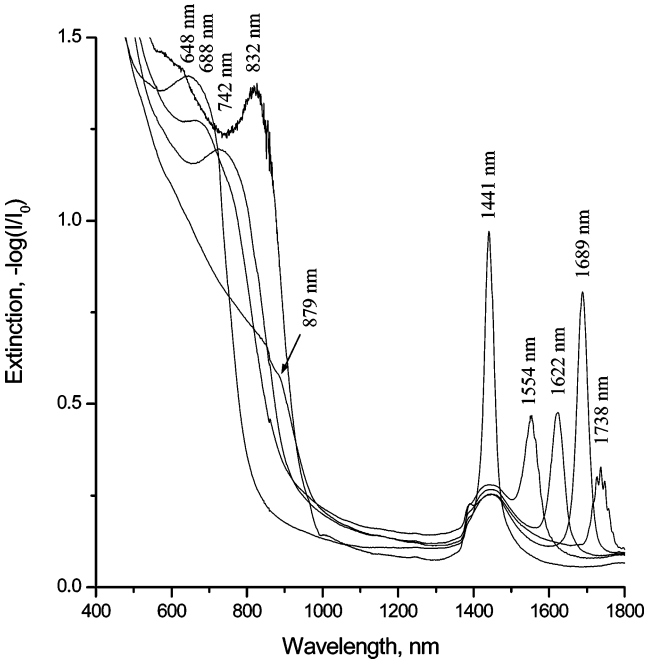

Figure 5. Normal incident extinction spectra of a 125-μm-thick CCA at different particle concentrations. The SiO_2 colloidal spheres are about 620 nm in diameter.

ion-exchange resin to substitute cationic and anionic ions with H^+ and OH^- and, as a result, these purified SiO_2 colloids readily self-assemble to form CCAs.

Figures 4 and 5 illustrate the transmission extinction spectra of SiO_2 CCA suspensions at normal light incidence. The thickness of the CCA was 125 μm placed between two quartz plates. In all the spectra, a broad band centered around 1440 nm is attributive to water absorption. The sharp peaks in 1200−1500 nm region for 403-nm SiO_2 spheres and in 1400−1800 nm region for 620-nm SiO_2 spheres result from the first-order Bragg diffraction of light by the CCAs. The maximum diffraction wavelength depended on lattice spacing between charged particles in suspension or concentrations of the SiO_2 colloids. The diffraction peak positions approximately obey Bragg's law:

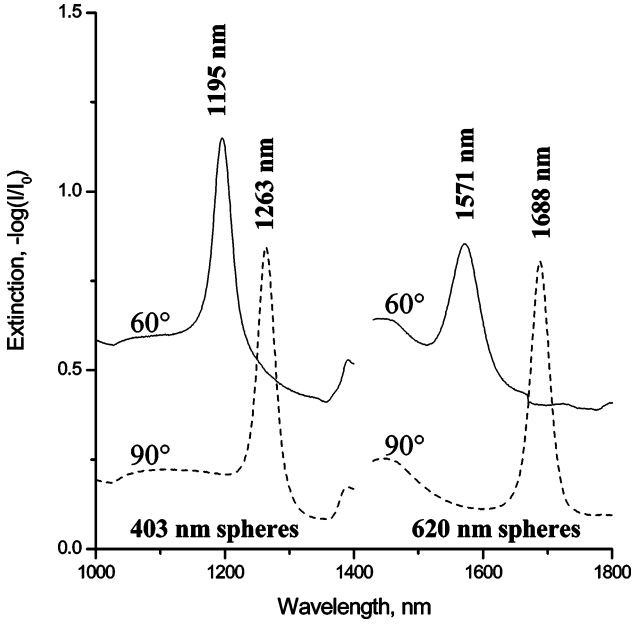

Figure 6. Extinction spectra of 403-nm and 620-nm SiO_2 CCAs at two different incident light angles.

$$m\lambda = 2nd \sin \theta \tag{1}$$

where m is the order of diffraction, λ is the diffracted wavelength in a vacuum, n is the effective refractive index of the system (including solvents and colloidal particles), d is the spacing between the diffracting planes, and θ is the Bragg glancing angle between the incident light propagation direction and the diffracting planes. The inter-planar spacing, d, can be expressed in terms of the unit cell parameter, a, and Miller indices:

$$d = a/(h^2 + k^2 + l^2)^{1/2} \tag{2}$$

The CCAs with FCC structure are usually oriented with their (111) planes parallel to the surface of the cell containing the CCA.[33] Multiple crystal planes can simultaneously satisfy the Bragg condition. By adjusting the d spacing of the photonic crystal (which was achieved by altering the volume fraction of the SiO_2 spheres in CCA dispersions by dilution), we were able to continuously tune the diffraction wavelengths in the NIR region from ~800 to ~1800 nm. Additionally, the diffraction peaks depend on incident light angles. By decreasing the incident light angle, we were able to tune the diffraction to low wavelength at fixed colloidal particle concentration (Figure 6). These properties allow the SiO_2 CCA to serve as a tunable optical filter in the NIR spectral region.

In addition to the sharp primary extinction peaks, the corresponding secondary extinction peaks were observed. In Figure 4, these secondary peaks are at 672, 658, 652, 637, and 618 nm relative to the primary peaks at 1451, 1405, 1296, 1264, and 1232 nm, respectively. Similarly in Figure 5, these secondary peaks were observed at 879, 832, 742, 688, and 648 nm relative to the primary peaks at 1738, 1689, 1622, 1554, and 1296 nm. These secondary peaks are located at approximately half of the wavelength of the first-order diffraction peaks. The secondary diffraction of the (111) plane and superposition of diffraction from the (200), (020), (002), (022), (202), and (220) planes [33] together give very broad bands in the visible spectral region.

These CCAs are very stable, even at very high particle concentrations. Their diffraction properties can remain un-

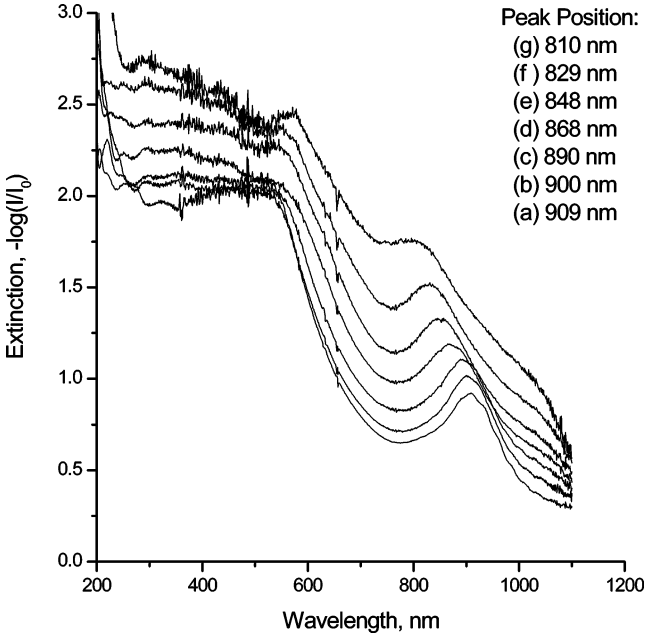

Figure 7. Extinction spectra of close-packed SiO_2 particle−air array at different incident light angles: (a) 90°, (b), 82.5°, (c) 75°, (d) 67.5°, (e) 60°, (f) 52.5°, and (g) 45°. The SiO_2 particle size is 403 nm and the SiO_2 particle−air array thickness is 50 μm.

changed for years, if placing the sample in closed containers at room temperature. By evaporating water in CCA, the SiO_2 particle density increases with a blue-shift of diffracted wavelength until forming a close-packed SiO_2 particle−air array. The dried thin films of colloidal photonic crystals still retain the optical diffraction property. Thickness of the thin film can be confined by an optical path thickness of quartz cell in 25−125 μm. In Figure 7, it is clear that the diffraction band of a 50-μm-thick thin film of 403-nm SiO_2 particles gradually shifts to blue wavelength with decreasing angle between the incident light and the particle thin film surface from 90° to 45°.

It is also important to note that the diffractions prevented any lights from transmitting through the CCAs and the close-packed SiO_2 particle−air arrays below ~550 nm spectral region (Figures 4−7, but not shown in Figure 6). Since SiO_2 colloids themselves do not absorb lights in the visible spectral region, the SiO_2 CCAs and the close-packed SiO_2 particle−air arrays function like photonic band gap (PBG)[35] crystal materials, although the FCC crystal geometry and the low refractive index difference between SiO_2 spheres ($n = 1.45$) and water ($n = 1.33$) or air ($n = 1.0$) are not expected to give full band gaps.[35] In comparison with a theoretically expected perfect lattice, the imperfect SiO_2 CCAs and close-packed SiO_2 particle−air arrays with local disorders may cause a broadened diffraction[33] which is likely to result in the formation of the PBG. If the broadened diffraction bands from all high Miller index planes overlap, it is possible that light is diffracted at all incident angles for all wavelengths below a certain cutoff. Therefore, our observations perhaps demonstrate that a pseudo full PBG exists for light at wavelengths below 550 nm for the SiO_2 photonic crystals.

To the best of our knowledge, this is the first report showing the NIR diffractions at wavelength >1500 nm using SiO_2 colloidal photonic crystals, although diffraction properties of SiO_2 photonic crystals have been widely studied. Compared to polystyrene or other polymeric colloids, the SiO_2 colloids offer several advantages for industrial applications because of their stability in a wide range of solvents, and their chemical and thermo resistance. The unique diffraction properties of SiO_2 CCAs in NIR spectral region give it potential applications as tunable NIR optical filters and/or as PBG materials in the UV−visible spectral region.

Acknowledgment. This research was partially supported by the Office of Basic Energy Sciences, U.S. Department of Energy, under Contract DE-AC05-00OR22725 with Oak Ridge National Laboratory, which is managed by UT-Battelle LLC. Wei Wang thanks Dr. Sanford A. Asher of the Department of Chemistry, University of Pittsburgh, for his helpful guidance in part of the colloid synthesis.

References and Notes

(1) Xia, Y.; Gates, B.; Li, Z. Y. *Adv. Mater*. **2001**, *13*, 409.
(2) Asher, S. A.; Holtz, J.; Weissman, J.; Pan, G. S. *MRS. Bull*. **1998**, *23*, 44.
(3) Jiang, P.; Bertone, J. F.; Colvin, V. L. *Science* **2001**, *291*, 453.
(4) Velev, O. D.; Kaler, E. W. *Adv. Mater*. **2000**, *12*, 531.
(5) Norris, D. J.; Vlasov, Y. A. *Adv. Mater*. **2001**, *13*, 371.
(6) Yoshiyama, T.; Sogami, I. *Phys. Rev. Lett*. **1984**, *53*, 2153.
(7) Monovoukas, Y.; Gast, A. P. *Langmuir* **1991**, *7*, 460.
(8) Wang, W.; Gu, B.; Liang, L.; Hamilton, W. *J. Phys. Chem. B* **2003**, *107*, 3400.
(9) Liu, L.; Li, P. S.; Asher, S. A. *Nature* **1999**, *397*, 141.
(10) Imhof, A.; van Blaaderen, A.; Maret, G.; Mellema, J.; Dhont, J. K. G. *J. Chem. Phys*. **1994**, *100*, 2170.
(11) Smits, C.; van Duijneveldt, J. S.; Dhont, J. K.; Lekkerkerker, H. N. W. *Phase Transitions* **1990**, *21*, 157.
(12) Flaugh, P. L.; O'Donnell, S. E.; Asher, S. A. *Appl. Spectrosc.* **1984**, *38*, 847.
(13) Reese, C. E.; Asher, S. A. *J. Colloid Interface Sci*. **2002**, *248*, 41.
(14) Jiang, P.; Bertone, J. F.; Hwang, K. S.; Colvin, V. L. *Chem. Mater*. **1999**, *11*, 2132.
(15) Comoretto, D.; Cavallo, D.; Dellepiane, G.; Grassi, R.; Marabelli, F.; Andreani, L. C.; Brabec, C. J.; Andreev, A.; Zakhidov, A. A. *Mater. Res. Soc. Symp. Proc*. **2002**, *708*, 317.
(16) Szekeres, M.; Kamalin, O.; Schoonheydt, R. A.; Wostyn, K.; Clays, K.; Persoons, A.; Dékány, I. *J. Mater. Chem*. **2002**, *12*, 3268.
(17) Reculusa, S.; Ravaine, S. *Chem. Mater*. **2003**, *15*, 598.
(18) Stöber, W.; Fink, A.; Bohn, E. *J. Colloid Interface Sci.* **1968**, *26*, 62.
(19) Roberts, J. M.; Linse, P.; Osteryoung, J. G. *Langmuir* **1998**, *14*, 204.
(20) Zerda, T. W.; Hoang, G. *Chem. Mater.* **1990**, *2*, 372.
(21) Tan, C. G.; Bowen, B. D.; Epstein, N. *J. Colloid Interface Sci*. **1987**, *118*, 290.
(22) Matijević, E. *Langmuir* **1994**, *10*, 8.
(23) Bogush, G. H.; Tracy, M. A.; Zukoski, C. F., IV. *J. Non-Cryst. Solids* **1988**, *104*, 95.
(24) Van Blaaderen, A.; Vrij, A. In *Advances in Chemistry*, Series 234; Bergna, H. E., Ed.; American Chemical Society: Washington, DC, 1994; pp 83−111.
(25) Iler, R. K. *The Chemistry of Silica*; Wiley-Interscience: New York, 1979.
(26) Krieger, I. M.; O'Neill, F. M. *J. Am. Chem. Soc.* **1968**, *90*, 3114.
(27) Hiltner, P. A.; Papir, Y. S.; Krieger, I. M. *J. Phys. Chem.* **1971**, *75*, 1881.
(28) Okubo, T. *J. Chem. Soc., Faraday Trans. 1* **1986**, *82*, 3163.
(29) Ito, K.; Nakamura, H.; Ise, N. *J. Chem. Phys.* **1986**, *85*, 6136.
(30) Monovoukas, Y.; Gast, A. P. *J. Colloid Interface Sci*. **1989**, *128*, 533.
(31) Kesavamoorthy, R.; Tandon, S.; Xu, S.; Jagannathan, S.; Asher, S. A. *J. Colloid Interface Sci*. **1992**, *153*, 188.
(32) Asher, S. A.; Holtz, J.; Liu, L.; Wu, Z. *J. Am. Chem. Soc*. **1994**, *116*, 4997.
(33) Liu, L.; Li, P.; Asher, S. A. *J. Am. Chem. Soc*. **1997**, *119*, 2729.
(34) Woodcock, L. V. *Nature* **1997**, *385*, 141.
(35) Joannopoulos, J. D.; Meade, R. D.; Winn, J. N. *Photonic Crystals−Molding the Flow of Light*; Princeton University Press: Princeton, 1995; Chapter 6.